# Divergent Synthesis of Indolenine and Indoline Ring Systems by Palladium-Catalyzed Asymmetric Dearomatization of Indoles

Dong Gao and Prof. Dr. Lei Jiao*

**Abstract:** Dearomatized indole derivatives bearing a C3- or C2-stereocenter exist ubiquitously in natural products and biologically active molecules. Despite remarkable advances in their chemical synthesis, stereoselective and *regio*-divergent methods are still in a high demand. Herein, a Pd-catalyzed intermolecular asymmetric spiroannulation of 2,3-disubstituted indoles with internal alkynes has been developed for the efficient construction of indoline structures with a C2-quaternary stereocenter. Stereospecific aza-semipinacol rearrangement of these indoline derivatives under acidic conditions afforded indolenine products bearing a C3-quaternary stereocenter, where the selectivity for the rearranging group could be controlled by the reaction sequence. The asymmetric spiroannulation together with the subsequent aza-semipinacol rearrangement enabled a divergent access to dearomatized indole derivatives with either a C3- or a C2-quaternary stereocenter.

Indolenines bearing a C3-quaternary stereocenters and indolines bearing a C2-quaternary stereocenter are widely occurring core structures in many bioactive natural products and pharmaceutically active molecules (Figure 1).[1, 2b, 2d] The development of efficient synthetic methods that enable efficient construction of these core structures is of great significance.[2]

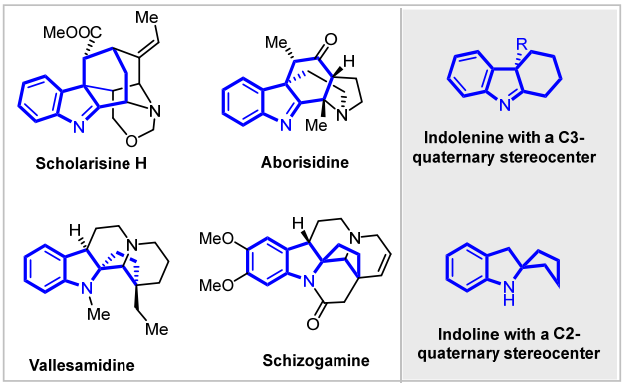


**Figure 1.** Representative indoline/indolenine alkaloids.

Catalytic asymmetric dearomatization (CADA) reactions serve as one of the most straightforward approach to chiral building blocks from aromatic substrates.[3] Recently, a series of CADA reactions have been developed for the construction of chiral indolenine/indoline derivatives based on the reactivity of C($sp^2$)-Pd species (Scheme 1).[4-6] The majority of these reactions were performed in an intramoleculcar manner (Scheme 1a), in which a haloarene or an acetylene is tethered to the N1-, C2- or C3-position of indole as the C($sp^2$)-Pd precursor. The You group achieved enantioselective C3-arylation of C3-tethered indoles;[4p] Jia[4b,4k] and Fukuyama[4n] developed the dearomative Heck reaction of N1- and C2-tethered indoles to build a C2-stereocenter; Jia,[4h-j,4m,4o] Liang,[4c,4d,4g] Lautens,[4h] and Dai[4e] reported the asymmetric dearomative difunctionalization of C2-tethered indoles by employing an external nucleophile.

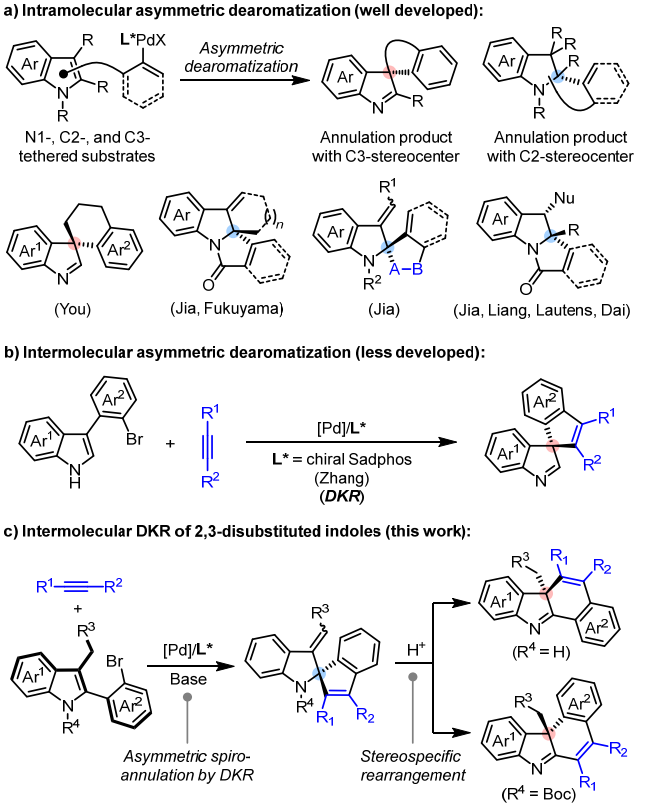


**Scheme 1.** Palladium-catalyzed asymmetric dearomatization of indoles involving a C($sp^2$)-Pd species. DKR = dynamic kinetic resolution.

Compared with intramolecular cyclization, the intermolecular version allows for a more divergent approach to dearomatized products. In this regard, Zhang and co-workers reported recently an enantioselective annulative dearomatization of C3-bromoarylindoles with alkynes using the Pd/Sadphos catalytic system to access various spiro-indolenines with a C2-quaternary stereocenter (Scheme 1b).[5] However, to date the intermolecular asymmetric dearomatization of C2-arylindoles has not been reported yet, and stereoselective construction of structurally diversified indoline/indolenine derivatives remains a formidable challenge.[7]

Herein, we report a Pd-catalyzed asymmetric intermolecular spiroannulation reaction of C2-arylindoles with internal alkynes, leading to the formation of spiro-indolines bearing a C2-quaternary stereocenter (Scheme 1c). These products could undergo a stereospecific aza-semipinacol rearrangement under acidic conditions, affording fused-indolenines with a C3-quaternary stereocenter. Furthermore, the

[*] D. Gao, Prof. Dr. L. Jiao
Center of Basic Molecular Science (CBMS), Department of Chemistry, Tsinghua University, Beijing 100084, China
E-mail: Leijiao@mail.tsinghua.edu.cn

Supporting information for this article is given via a link at the end of the document.

migration selectivity of this process could be tuned by the selection of reaction sequence. The asymmetric spiroannulation together with the stereospecific rearrangement enabled a divergent access to dearomatized indole derivatives with either a C3- or a C2-quaternary stereocenter.

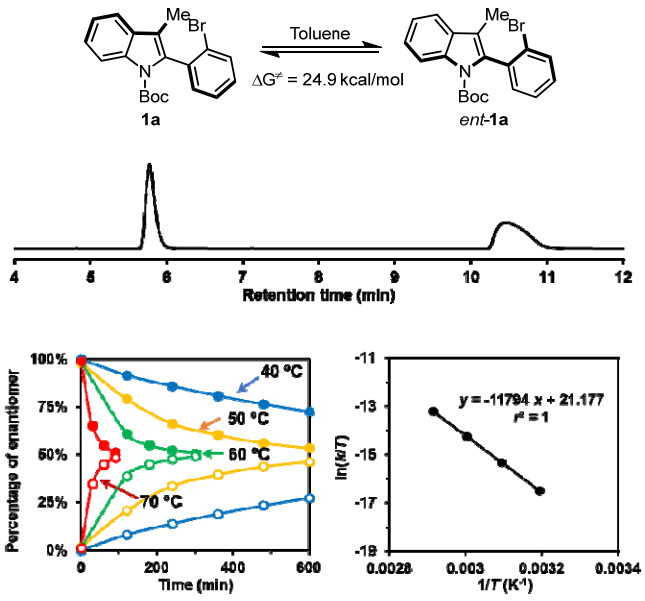


**Scheme 2.** Rotational Barrier Determination for Substrate **1a**

At the outset, we envisioned to attempt the reaction between Boc-protected 2-(2-bromophenyl)-3-methyl-1*H*-indole (**1a**) and acetylenes as a model reaction. We first focused on the aryl-aryl rotational barrier of **1a**, since similar substrates exhibit axial chirality[5,6d] and the interconversion between the two enantiomers should be facile enough to ensure efficient dynamic kinetic resolution (DKR).[8] We found that, the enantiomers of **1a** could be well resolved by chiral HPLC, indicating that they interconvert slowly under room temperature (Scheme 2). The separation of both enantiomers allowed us to determine the kinetic parameters of the racemization process by performing the reaction under elevated temperatures.[9] We found that, under 70 ºC the racemization process completed within 100 min. On the basis of the measured enantiomerization rate constants [*k*(T)], the enantiomerization barrier of **1a** was determined to be 24.9 kcal/mol at 298 K by applying the Erying equation, which ensures a rapid racemization process at elevated temperature.

Bearing this information in mind, we commenced the study on the reaction between **1a** and diphenylacetylene (**2a**) by employing $Pd(dba)_2$ as the precatalyst and toluene as the solvent (Table 1). It was found that, chiral NHC ligand **L1**, BINAP (**L2**), spiro-phosphoramidite ligand **L3**, and Feringa-type ligand **L4** resulted in unsatisfactory results (entries 1-4). To our delight, a promising result was observed by employing the Carreira ligand **L5** with *t*-BuOLi as the base at 120 °C, affording product **3aa** in 55% $^1$H NMR yield with 92:8 er (entry 5). A better result was achieved by lowering the reaction temperature to 90 °C and switching the base to MeOLi, providing **3aa** in 88% isolated yield with 95:5 er (entry 9). Further optimization on ligand structure indicated that more sterically hindered ligands **L6** and **L7** exhibited a negative effect on enantioselectivity (entries 10-11). The fluoro-substituted ligand **L8** was found to give comparable yield and slightly inferior enantioselectivity (entry 12). A comparison showed that phosphoramidite ligand **L9** was inferior compared with **L5** (entry 13). The absolute configuration of product **3aa** was confirmed by the single crystal X-ray diffraction analysis.

**Table 1.** Optimization of the reaction conditions.

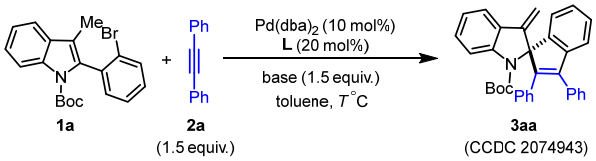


| Entry | Base | L | T/°C | Yield(%)[a] | Er[b] |
|---|---|---|---|---|---|
| 1[c] | *t*-BuONa | **L1** | 120 | 9 | 53.5:46.5 |
| 2[d] | $Cs_2CO_3$ | **L1** | 120 | 23 | 51.5:48.5 |
| 2[e] | $Cs_2CO_3$ | **L2** | 120 | 0 | - |
| 3[f] | *t*-BuOLi | **L3** | 120 | 75 | 54:46 |
| 4[g] | *t*-BuOLi | **L4** | 120 | 12 | 75.5:24.5 |
| 5 | *t*-BuOLi | **L5** | 120 | 55 | 92:8 |
| 6 | *i*-PrOLi | **L5** | 120 | 60 | 92:8 |
| 7 | MeOLi | **L5** | 120 | 65 | 93:8 |
| 8[h] | MeOLi | **L5** | 100 | 70 | 95:5 |
| 9 | MeOLi | **L5** | 90 | 88[i] | 95:5 |
| 10 | MeOLi | **L6** | 95 | 52 | 44:56 |
| 11 | MeOLi | **L7** | 95 | 20 | 46:54 |
| 12[i] | MeOLi | **L8** | 90 | 89 | 92:8 |
| 13[g] | *t*-BuOLi | **L9** | 120 | 52 | 54.5:45.5 |

[a] Determined by $^1$H NMR with $CH_2Br_2$ (0.1 mmol) as an internal standard. [b] Enantiomeric ratios were determined by chiral stationary phase HPLC. [c] Using $Pd(OAc)_2$ (10 mol%) as palladium source, KI (1.5 equiv) as additive, and Dioxane (0.1 M) as the solvent. [d] Using $[Pd(C_3H_5)Cl]_2$ (5 mol%) as palladium source, **L1** (15 mol%), and Dioxane (0.1 M) as the solvent. [e] Using $[Pd(C_3H_5)Cl]_2$ (2.5 mol%) and **L2** (7.5 mol%). [f] Using $Pd(dba)_2$ (5.0 mol%) and **L3** (7.5 mol%). [g] Using $Pd(dba)_2$ (10.0 mol%) and **L2** (15.0 mol%). [h] MeOH (1.0 equiv.) as additive. [i] Yield of isolated product.

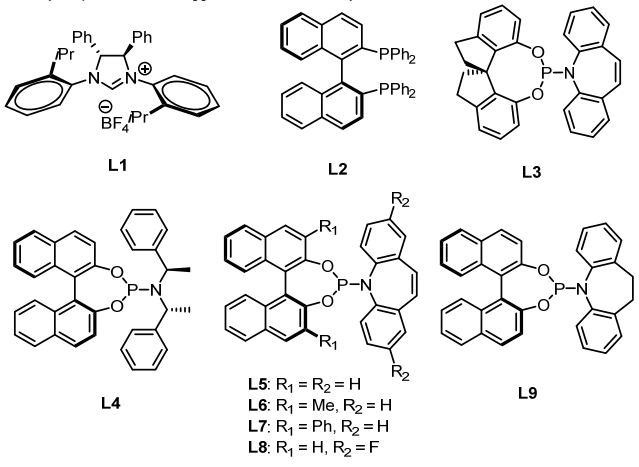

**Table 2.** Scope of Indole Substrates and Internal Alkynes[a]

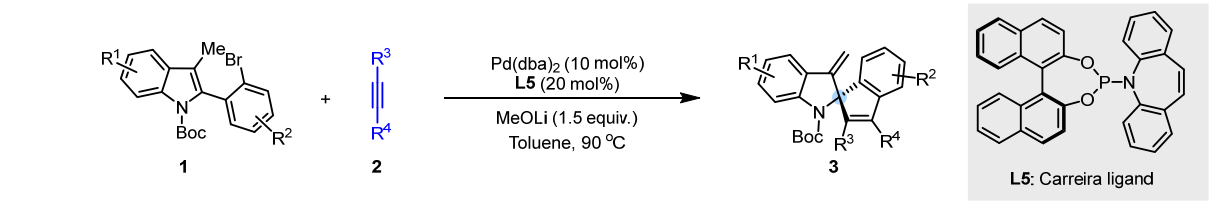


***Scope of indole substrate***

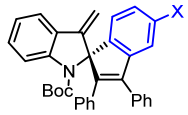

**3aa**, X = H, 88% yield, 95:5 er
**3ba**, X = F, 86% yield, 96:4 er
**3ca**, X = Cl, 73% yield, 96:4 er
**3da**, X = OMe, 70% yield, 90:10 er
**3ea**, X = Me, 86% yield, 94:6 er
**3fa**, X = $CF_3$, 23% yield, 92:8 er

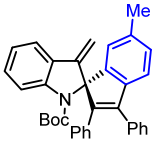

**3ga**
87% yield, 95:5 er

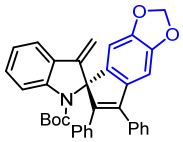

**3ha**
99% yield, 95:5 er

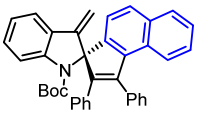

**3ia**
39% yield, 93:7 er

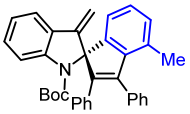

**3ja**
62% yield, 76:24 er

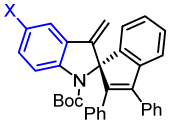

**3ka**, X = Me, 82% yield, 93:7 er
**3la**, X = $CF_3$, 33% yield, 94:6 er
**3ma**, X = Cl, 59% yield, 93:7 er

***Scope of acetylene component***

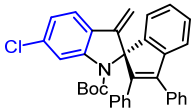

**3na**
64% yield, 95:5 er

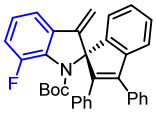

**3oa**
23% yield, 87:13 er

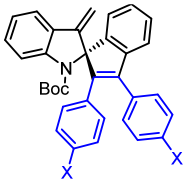

**3ab**, X = F, 96% yield, 94:6 er
**3ac**, X = Cl, 74% yield, 93.5:6.5 er
**3ad**, X = OMe, 97% yield, 94:6 er
**3ae**, X = $CF_3$, 57% yield, 92:8 er

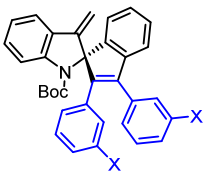

**3af**, X = F, 94% yield, 91.5:8.5 er
**3ag**, X = OMe, 93% yield, 95:5 er

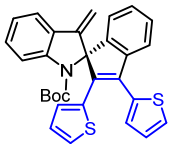

**3ah**
16% yield, 91:9 er

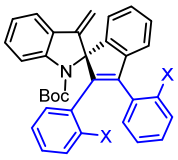

**3ai**, X = F, 46% yield, 77:23 er
**3aj**, X = Me, 0% yield

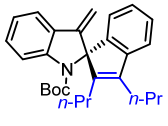

**3ak**
91% yield, 92:8 er
*[98%, 90:10 er on 1.3 g scale]*

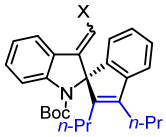

**3pk**, X = Me, 95% yield, *Z*/*E* = 1:12, (*Z*)-**3pk**: 90:10 er, (*E*)-**3pk**: 88:12 er
**3qk**, X = $CO_2{}^tBu$, 55% yield, *Z*/*E* = 1:12, (*Z*)-**3qk**: 83:17 er, (*E*)-**3qk**: 88:12 er

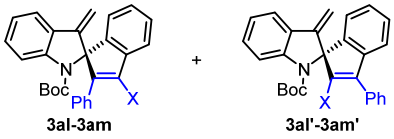

**3al-3am**

**3al'-3am'**

**3al/3al'**, X = $CH_2OTBS$
**3al**, 78% yield, 94:6 er
**3al'**, 16% yield, 93.5:6.5 er
**3am/3am'**, X = Me
**3am**, 83% yield, 89:11 er
**3am'**, 15% yield, 77:23 er

[a] Reaction conditions: **1** (1.0 equiv), **2** (1.5 equiv), and toluene (0.1 M) under Ar. Yields of isolated products are reported. The *Z*/*E* ratios of **3pk** and **3qk** were determined by crude $^1$H NMR. The er values were determined by chiral HPLC.

To illustrate the generality of the reaction, the scope of indole coupling partners (**1a-o**) was initially investigated (Table 2). Gratifyingly, indole substrates with fluoro, chloro, methoxyl, and methyl substituents (**1b-e**) at the 5-position worked well under the optimal reaction conditions, giving the corresponding spiro-indoline products **3ba-3ea** in 70-86% yield with 90:10 to 96:4 er. Substrate bearing an electron-withdrawing trifluoromethyl group (**1f**) was also tolerated to afford **3fa** in 92:8 er, whereas the reaction yield decreased to 23%. The substrates containing 6-methyl, methylenedioxy, and more sterically congested naphthyl group (**1g-i**) reacted smoothly to provide the desired products **3ga-3ia** in 39-99% yield with 93:7-95:5 er. However, introduction of a methyl group at the 6-position (**3ja**) of the phenyl moiety only gave desired product in 76:24 er. Moreover, substituents on the indole moiety (5'-methyl, 5'-trifluoromethyl, 5'-chloro, 6'-chloro) of the substrates (**1k-n**) were compatible with the reaction, delivering **3ka-3na** in 33-82% yield with 93:7-95:5 er. Compound **3oa** could only be obtained in 23% yield and 87:13 er by using a 7-fluoro substituted indole substrate.

Having evaluated the scope of 2-arylindoles, we then concentrated on the scope of the internal alkyne (Table 2). Symmetrical diaryl acetylenes with various substituents at the *para*- (**2b-e**) or *meta*- (**2f-g**) position of both phenyl rings participated in the reaction smoothly to give the

corresponding products **3ab-3ag** in 57-97% yield with 92:8-95:5 er. Di(thiophen-2-yl)acetylene (**2h**) could undergo the reaction with **1a**, but afforded a low yield of cyclization product **3ah** in 91:9 er. The *ortho*-substituent on the aryl groups of diarylacetylene generally exhibited a negative effect on the reaction: *ortho*-fluoro substituted 1,2-bis(2-fluorophenyl)ethyne **2i** afforded product **3ai** in a moderate yield with a poor enantioselectivity (77:23 er), and no desired product was observed for the more sterically hindered *ortho*-methyl substituted diphenylacetylene **2j**. To our delight, the symmetrical dipropylacetylene **2k** was found to be suitable to undergo the annulation with substrates **1a**, **1p**, and **1q**. Notably, a gram-scale synthesis of **3ak** (1.31 g) was carried out to afford the product in 98% yield with 90:10 er, indicating the scalability of the present method.

**Table 3.** Aza-semipinacol rearrangement[a]

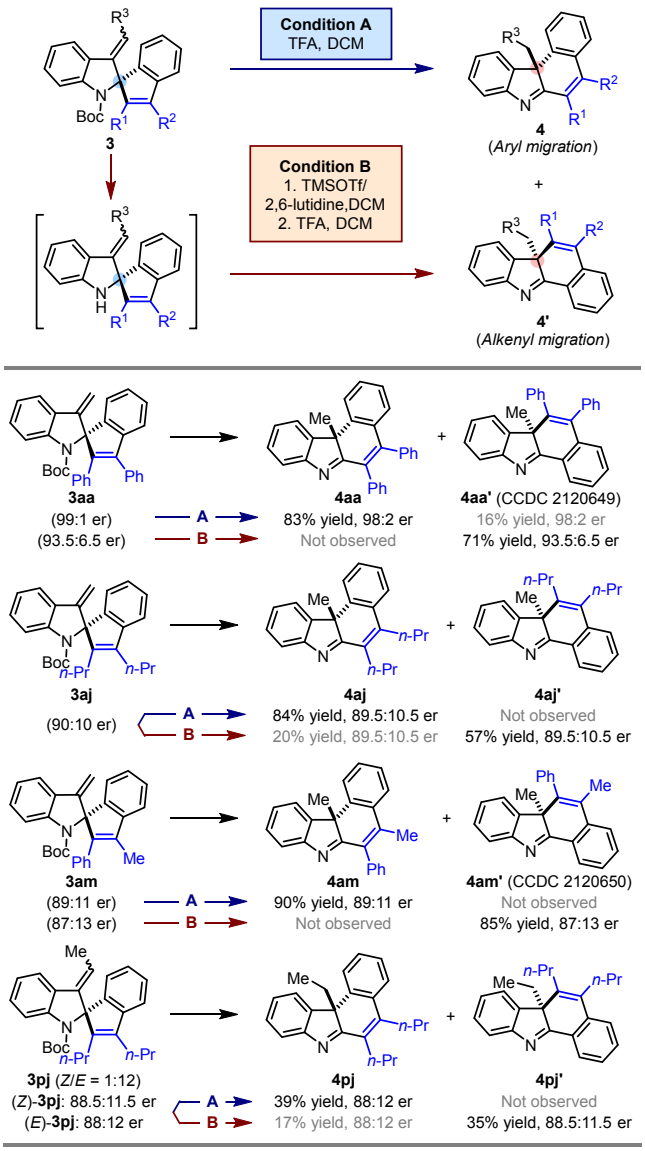


[a] Condition A: TFA/DCM = (1:10 v/v) (0.1 M). Condition B: 1. TMSOTf (4.0 equiv), 2,6-lutidine (5.0 equiv), DCM (0.1 M) 2. TFA/DCM = (1:10 v/v) (0.1 M). Yields of isolated product are reported. The *er* values were determined by chiral HPLC. TFA = trifluoroacetic acid, TMSOTf = trimethylsilyl trifluoromethanesulphonate.

Moreover, the presence of an ethyl group (**1p**) or a *tert*-butoxycarbonylmethyl (**1q**) at C3-position of the indole ring led to the corresponding products **3pk** and **3qk** in good yields and enantioselectivities. Finally, the unsymmetrical alkyl/aryl mixed acetylenes **2l** and **2m** produced cyclization products in good yields with decent enantioselectivities and satisfactory regioselectivities.

The existence of the C2-spiroindoline structure in the cyclized products enabled a potential aza-semipinacol rearrangement[4f, 10] leading to the formation of a C3-stereocenter, and if the rearrangement proceeded stereospeficially, enantioenriched C3-substituted indolenine derivative could be obtained. Therefore, we attempted to perform an acid-promoted aza-semipinacol rearrangement on the spiroindoline products (Table 3). We found that, by treating the C3-methylene (**3aa**, **3aj**, **3am**) or C3-ethylidene (**3pj**) substituted spiro-indolines with TFA (Condition A), the rearranged products bearing a C3-quaternary stereocenter (**4aa**, **4aj**, **4am**, and **4pj**) were obtained in moderate to excellent overall yield without loss of enantiopurities. In this process both the cleavage of the *N*-Boc group and the stereospecific rearrangement of the C2-substituent proceeded smoothly, and the aryl migration was favored over the alkenyl migration.

To figure out whether the rearrangement step occurs prior to or after the elimination of the *N*-Boc group, we investigated another reaction sequence involving stepwise deprotection and rearrangement for the same set of C2-spiroindoline derivatives (Condition B). The deprotection of *N*-Boc group proceeded smoothly by treatment with TMSOTf/2,6-lutidine, and the crude deprotected product was treated with TFA as before. To our surprise, this reaction sequence delivered alkenyl migration product (**4aa', 4aj', 4am', 4pj'**) as the major product with complete retention of enantiopurities. This result indicates that the nature of the *N*-substituent has a remarkable effect on the aza-semipinacol rearrangement, and under Condition A the rearrangement occurred prior to deprotection. Therefore, by choosing an appropriate reaction sequence, rearrange of C2-spiroindoline to C3-substituted indolenine with selective aryl/alkenyl migration could be achieved.

In order to gain more mechanistic insights into the palladium-catalyzed cascade spiroannulation, we performed a DFT computational study. The reaction between 2,3-disubstituted indole **1a** and diphenylacetylene **1b** catalyzed by the combination of Pd/**L5** was selected as the model reaction, and the calculated reaction pathway is shown in Scheme 3. The Pd-ligand complex, Pd(**L5**)$_2$, was figured out to be the starting point of the catalytic cycle.[11] Ligand exchange with substrate **1a** forms the arene-coordinated intermediate **INT1**, which is significantly endergonic by 13.6 kcal/mol. **INT1** then undergoes oxidative addition via **TS1** ($\Delta G^{\neq}$ = 19.9 kcal/mol) to produce the Pd(II) intermediate **INT2**, in which the carbonyl of the Boc-group coordinates to the Pd center. After a slightly endergonic association of diphenylacetylene **2a** to form **INT3**, migratory insertion of coordinated acetylene into the Pd(II)-aryl bond proceeds through **TS2** ($\Delta G^{\neq}$ = 20.4 kcal/mol) to produce **INT4** in an irreversible manner, which fixes the axial chirality of the intermediate and thus determines the stereochemical outcome of the reaction. Subsequently, a facile intramolecular migratory insertion of the indole C2−C3 double bond into the Pd(II)-alkenyl bond via **TS3** ($\Delta G^{\neq}$ = 4.0 kcal/mol) to furnish intermediate **INT5**, which sets the C2-stereocenter dictated by the axial chirality of **INT4**. Finally, $\beta$-H elimination via **TS4** ($\Delta G^{\neq}$ = 8.2 kcal/mol) occurs to forge the C3-methylene moiety, and the following base-promoted dehydrobromination and substrate-product exchange releases the C2-spiroindoline product (*R*)-**3aa** while regenerating **INT1**.

It is notable that only the pathway leading to the (*R*)-enantiomer was depicted in Scheme 3. The other diastereomeric pathway leading to the (*S*)-product originates from the coordination of *ent*-**1a** with the Pd center to form the diastereomeric **INT1'**. However, due to high rotation energy barrier, the enantiomers of both **INT1** and **INT2** are not interconvertible

by C-C bond rotation (for **INT2**, the rotational barrier is calculated to be 35.4 kcal/mol, see SI for detail). Therefore the irreversible alkyne insertion step (via **TS2**) serves as the rate- and enantio-determining step of the reaction. The calculated $\Delta\Delta G^{\neq}$ [$\Delta G^{\neq}$(**TS2'**) - $\Delta G^{\neq}$(**TS2**)] is 1.1 kcal/mol, which is in agreement with the experimental observation that the reaction favored the formation of (*R*)-**3aa**. It is notable that the free energy barrier for the interconversion of atropisomers of **1a** was determined to be 24.9 kcal/mol (Scheme 2), while the activation free energy of the reaction was calculated to be 20.4 kcal/mol [from Pd(**L5**)$_2$ to **TS2**]. Given that the key transition structure **TS2** involves three components (catalyst, substrate **1a**, and alkyne **2a**), the corrected activation energy barrier according to their actual concentrations in the catalytic system (0.01 M, 0.1 M, and 0.15 M, respectively) is 25.6 kcal/mol, which accounts for the observed dynamic kinetic resolution.

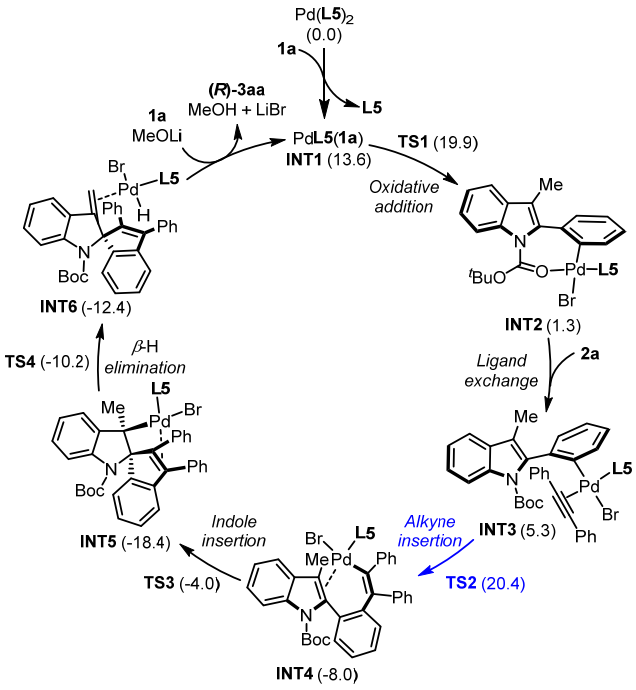


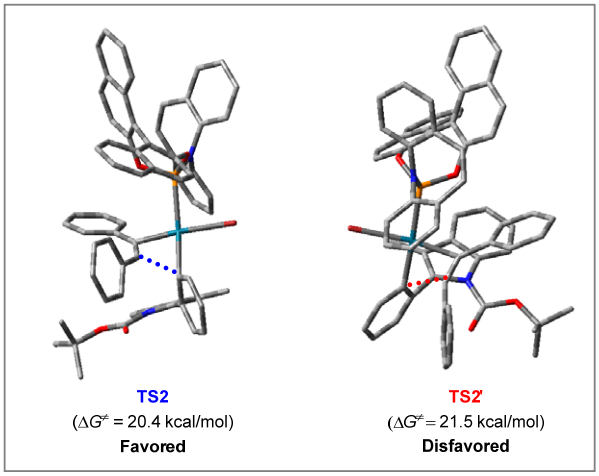


**Scheme 3.** DFT-calculated reaction pathway and the stereochemical model for the enantio-determining alkyne insertion step. DFT calculation were performed at the M06/6-311+g(d,p)/SDD//B3LYP/6-31g(d)/Lanl2dz level of theory, and relative Gibbs free energies in solution (toluene) were shown in parentheses.

In summary, we have developed a palladium-catalyzed enantioselective intermolecular dearomatization of C2-arylindoles with internal alkynes, leading to C2-spiroindolines bearing a C2-quaternary stereocenter with good yields and enantioselectivities. The stereospecific aza-semipinacol rearrangement afforded enantioenriched indolenine derivatives bearing a C3-quaternary stereocenter via an tunable aryl/alkenyl migration. The combined steps enabled a divergent access to dearomatized indole derivatives with either a C3- or a C2-quaternary stereocenter.

## Acknowledgements

The National Natural Science Foundation of China (Grant No. 21822304) are acknowledged for financial support. The technology platform of CBMS is acknowledged for providing instrumentation and computational resources. We also thank State Key Laboratory of Natural and Biomimetic Drugs for XRD analysis.

**Keywords:** spiro-indoline · indolenine · catalytic asymmetric dearomatization · stereospecific rearrangement · palladium catalysis

[1] For representative reviews, see: a) P. Ruiz-Sanchis, S. A. Savina, F. Albericio, M. Álvarez, *Chem. Eur. J.* **2011**, *17*, 1388-1408; b) S.-M. Li, *Nat. Prod. Rep.* **2010**, *27*, 57-78.

[2] For representative reviews and examples, see: a) T. S. Silva, M. T. Rodrigues, H. Santos Jr, L. A. Zeoly, W. P. Almeida, R. C. Barcelos, R. C. Gomes, F. S. Fernandes, F. Coelho, *Tetrahedron* **2019**, *75*, 2063-2097; b) J. Bariwal, L. G. Voskressensky, E. V. Van der Eycken, *Chem. Soc. Rev.* **2018**, *47*, 3831-3848; c) J. Song, D.-F. Chen, L.-Z. Gong, *Natl. Sci. Rev.* **2017**, *4*, 381-396; d) M. J. James, P. O'Brien, R. J. Taylor, W. P. Unsworth, *Chem. Eur. J.* **2016**, *22*, 2856-2881; e) J. D. Podoll, Y. Liu, L. Chang, S. Walls, W. Wang, X. Wang, *Proc. Natl. Acad. Sci. U. S. A.* **2013**, *110*, 15573-15578; f) M. Bandini, A. Eichholzer, *Angew. Chem. Int. Ed.* **2009**, *48*, 9608-9644; *Angew. Chem.* **2009**, *121*, 9786-9824.

[3] For representative reviews, see: a) Z. Wang, *Org. Biomol. Chem.* **2020** , *18*, 4354-4370; b) C. Zheng, S.-L. You, *Nat. Prod. Rep.* **2019**, *36*, 1589-1605; c) J. M. Saya, E. Ruijter, R. V. A. Orru, *Chem. Eur. J.* **2019**, *25*, 8916-8935; d) J. B. Chen, Y. X. Jia, *Org. Biomol. Chem.* **2017**, *15*, 3550-3567; e) C. Zheng, S.-L. You, *Chem* **2016**, *1*, 830-857; f) W. T. Wu, L. Zhang, S.-L. You, *Chem. Soc. Rev.* **2016**, *45*, 1570-1580; g) S. P. Roche, J.-J. Youte Tendoung, B. Tréguier, *Tetrahedron* **2015**, *71*, 3549-3591; h) C. X. Zhuo, C. Zheng, S.-L. You, *Acc. Chem. Res.* **2014**, *47*, 2558-2573; i) C. X. Zhuo, W. Zhang, S.-L. You, *Angew. Chem. Int. Ed.* **2012**, *51*, 12662-12686; *Angew. Chem.* **2012**, *124*, 12834-12858; For a book, see: j) S.-L. You, *Asymmetric Dearomatization Reactions,* VCH, Weinheim, **2016**.

[4] For a review, see: a) N. Zeidan, M. Lautens, *Synthesis* **2019**, *51*, 4137-4146. For representative examples, see: b) R.-X. Liang, L.-J. Song, J.-B. Lu, W.-Y. Xu, C. Ding, Y.-X. Jia, *Angew. Chem. Int. Ed.* **2021**, *60*, 7412-7417; *Angew. Chem.* **2021**, *133*, 7488-7493; c) Y. Li, H.-Y. Zhang, Y. Zhang, Y.-P. Han, J. Zhao, Y.-M. Liang, *J. Org. Chem.* **2021**, *86*, 14640-14651; d) Y. Li, Yue-Su, H.-Y. Zhang, Y. Zhang, Dong-Han, Y.-P. Han, J. Zhao, Y.-M. Liang, *ChemistrySelect* **2021**, *6*, 4719-4724; e) M.-L. Han, W. Huang, Y.-W. Liu, M. Liu, H. Xu, H. Xiong, H.-X. Dai, *Org. Lett.* **2021**, *23*, 172-177; f) D. Gao, L. Jiao, *J. Org. Chem.* **2021**, *86*, 5727-5743; g) Z. Zhang, B.-S. Zhang, K.-L. Li, Y. An, C. Liu, X.-Y. Gou, Y.-M. Liang, *J. Org. Chem.* **2020**, *85*, 7817-7839; h) C. Shen, N. Zeidan, Q. Wu, C. B. J. Breuers, R.-R. Liu, Y.-X. Jia, M. Lautens, *Chem. Sci.* **2019**, *10*, 3118-3122; i) R.-X. Liang, K. Wang, Q. Wu, W.-J. Sheng, Y.-X. Jia, *Organometallics* **2019**, *38*, 3927-3930; j) R.-X. Liang, R.-Z. Yang, R.-R. Liu, Y.-X. Jia, *Org. Chem. Front.* **2018**, *5*, 1840-1843; k) X. Li, B. Zhou, R.-Z. Yang, F.-M. Yang, R.-X. Liang, R.-R. Liu, Y.-X. Jia, *J. Am. Chem. Soc.* **2018**, *140*, 13945-13951; l) X. Qin, M. W. Y. Lee, J. S. Zhou, *Angew. Chem. Int. Ed.* **2017**, *56*, 12723-12726; *Angew. Chem.* **2017**, *129*, 12897-12900; m) R.-R. Liu, Y.-G. Wang, Y.-L. Li, B.-B. Huang, R.-X. Liang, Y.-X. Jia, *Angew. Chem. Int. Ed.* **2017**, *56*, 7475-7478; *Angew. Chem.* **2017**, *129*, 7583-7586; n) K. Douki, H. Ono, T. Taniguchi, J. Shimokawa, M. Kitamura, T. Fukuyama, *J. Am. Chem. Soc.* **2016**, *138*, 14578-14581; o) C. Shen, R.-R. Liu, R.-J. Fan, Y.-L. Li, T.-F. Xu,

J.-R. Gao, Y.-X. Jia, *J. Am. Chem. Soc.* **2015**, *137*, 4936-4939; p) K.-J. Wu, L.-X. Dai, S.-L. You, *Org. Lett.* **2012**, *14*, 3772-3775.

[5] H. Chu, J. Cheng, J. Yang, Y.-L. Guo, J. Zhang, *Angew. Chem. Int. Ed.* **2020**, *59*, 21991-21996; *Angew. Chem.* **2020**, *132*, 22175-22180.

[6] In addition to indole, this CADA strategy could also be extended to OH- or NH-containing electron-rich aromatic substrates. For selected examples, see: a) X. Mu, H. Yu, H. Peng, W. Xiong, T. Wu, W. Tang, *Angew. Chem. Int. Ed.* **2020**, *59*, 8143-8147; *Angew. Chem.* **2020**, *132*, 8220-8224; b) L. Fan, J. Liu, L. Bai, Y. Wang, X. Luan, *Angew. Chem. Int. Ed.* **2017**, *56*, 14257-14261; *Angew. Chem.* **2017**, *129*, 14445-14449; c) L. Bai, Y. Yuan, J. Liu, J. Wu, L. Han, H. Wang, Y. Wang, X. Luan, *Angew. Chem. Int. Ed.* **2016**, *55*, 6946-6950; *Angew. Chem.* **2016**, *128*, 7060-7064; d) L. Yang, H. Zheng, L. Luo, J. Nan, J. Liu, Y. Wang, X. Luan, *J. Am. Chem. Soc.* **2015**, *137*, 4876-4879; e) K. Du, P. Guo, Y. Chen, Z. Cao, Z. Wang, W. Tang, *Angew. Chem. Int. Ed.* **2015**, *54*, 3033-3037; *Angew. Chem.* **2015**, *127*, 3076-3080; f) R.-Q. Xu, Q. Gu, W.-T. Wu, Z.-A. Zhao, S.-L. You, *J. Am. Chem. Soc.* **2014**, *136*, 15469-15472; g) S. Rousseaux, J. García-Fortanet, M. A. Del Aguila Sanchez, S. L. Buchwald, *J. Am. Chem. Soc.* **2011**, *133*, 9282-9285; h) J. García-Fortanet, F. Kessler, S. L. Buchwald, *J. Am. Chem. Soc.* **2009**, *131*, 6676-6677.

[7] a) G. L. Trammel, R. Kuniyil, P. F. Crook, P. Liu, M. K. Brown, *J. Am. Chem. Soc.* **2021**, *143*, 16502-16511; b) P. Yang, R.-Q. Xu, C. Zheng, S.-L. You, *Chin. J. Chem.* **2020**, *38*, 235-241; c) Z. Liu, J. Chen, H.-X. Lu, X. Li, Y. Gao, J. R. Coombs, M. J. Goldfogel, K. M. Engle, *Angew. Chem. Int. Ed.* **2019**, *58*, 17068-17073; *Angew. Chem.* **2019**, *131*, 17224-17229.

[8] V. Bhat, E. R. Welin, X. Guo, B. M. Stoltz, *Chem. Rev.* **2017**, *117*, 4528-4561.

[9] F. Ceccacci, G. Mancini, P. Mencarelli, C. Villani, *Tetrahedron: Asymmetry* **2003**, *14*, 3117-3122.

[10] a) Q. Wang, J. Hu, N. Zheng, *Org. Lett.* **2019**, *21*, 614-617; b) Y. Yu, J. Li, L. Jiang, J.-R. Zhang, L. Zu, *Angew. Chem. Int. Ed.* **2017**, *56*, 9217-9221; *Angew. Chem.* **2017**, *129*, 9345-9349; c) Y. Yu, G. Li, L. Jiang, L. Zu, *Angew. Chem. Int. Ed.* **2015**, *54*, 12627-12631; *Angew. Chem.* **2015**, *127*, 12818-12822.

[11] B. Zhou, H. Wang, Z.-Y. Cao, J.-W. Zhu, R.-X. Liang, X. Hong, Y.-X. Jia, *Nat. Commun.* **2020**, *11*, 4380.

[12] Deposition Number 2074943 (for **3aa**), 2120649 (for **4aa'**), and 2120650 (for **4am'**) contains the supplementary crystallographic data for this paper. These data are provided free of charge by the joint Cambridge Crystallographic Data Centre and Fachinformationszentrum Karlsruhe Access Structures service www.ccdc.cam.ac.uk/structures.